BIOCHEMISTRY
including biophysical chemistry & molecular biology
Article

Biochemistry **2009,** *48,* 5313–5319 5313
DOI: 10.1021/bi900498z

An Unusually Stable G-Quadruplex within the 5′-UTR of the MT3 Matrix Metalloproteinase mRNA Represses Translation in Eukaryotic Cells

Mark J. Morris and Soumitra Basu*

Department of Chemistry, Kent State University, Kent, Ohio 44242

Received March 23, 2009; Revised Manuscript Received April 24, 2009

ABSTRACT: MT3-MMP is a matrix metalloproteinase involved in the regulation of cancer cell invasion and metastasis. The MT3-MMP mRNA contains a 20-nucleotide G-rich region (M3Q) upstream of the initiation codon. Herein, we report that the M3Q purine-only sequence forms an extremely stable intramolecular G-quadruplex structure and has an inhibitory role on translation of a reporter gene in eukaryotic cells. The formation of the G-quadruplex structure was indicated by circular dichroism (CD) spectroscopy and enzymatic footprinting with RNase T1. The unusual stability of the G-quadruplex was evidenced when addition of only 1 mM KCl resulted in about a 30 °C increase in the melting temperature (T_m), as compared to that obtained in the absence of added salt. The T_m was independent of the RNA concentration, suggesting an intramolecular G-quadruplex structure. Additionally, in a dual luciferase reporter assay performed in eukaryotic cells, the M3Q motif present in the context of the entire 5′-UTR of MT3-MMP repressed activity of its downstream gene by more than half. To the best of our knowledge, the naturally occurring M3Q sequence forms one of the most stable, intramolecular RNA G-quadruplexes reported. This report is the first to establish a functional role of a G-quadruplex forming sequence within the MT3-MMP 5′-UTR in the regulation of translation in eukaryotic cells.

G-Quadruplexes are four-stranded structures formed by guanine-rich sequences (*1*). The existence of a G-quartet structure composed of four hydrogen-bonded guanines was suggested more than four decades ago (*2*). The earliest reports of G-quadruplex structures comprising several quartets were limited mostly to the telomeres found at the end of chromosomes (*3*−*6*). Recent research has found that G-rich sequences are prevalent throughout the entire human genome (*7*, *8*), with a particular high frequency of occurrence in the promoter regions of genes (*9*), including some of the key growth regulatory genes and oncogenes, such as C-MYC, BCL2, VEGF, and KRAS (*10*−*14*).

Although DNA G-quadruplexes have been studied extensively, formation of RNA G-quadruplexes, particularly their regulatory roles in translational control, is just beginning to emerge. There is no apparent physicochemical barrier toward RNA G-quadruplex formation (*15*, *16*). It is logical to assume that the formation of RNA G-quadruplexes is more facile than formation of their DNA counterparts because RNA G-quadruplexes have been found to be more stable in the folded form (*15*, *17*, *18*) and do not have to compete with a complementary strand. In fact, it has been suggested that the 2′-OH group of RNA may have stabilizing effects on RNA G-quadruplexes, possibly through hydrogen bonding interactions (*17*, *19*).

RNA G-quadruplex-forming motifs have been found in the HIV-1 genomic RNA (*20*), FMR1 (*21*, *22*), FGF-2 (*23*), NRAS (*18*), Zic-1 (*24*), and IGF-II (*25*) mRNAs.[1] More interestingly, it has been shown that G-quadruplex-forming sequences present within the 5′-UTR can regulate translation in vitro as well as in vivo (*18*, *24*, *26*, *27*). A computational survey found putative G-quadruplex-forming sequences to be enriched within mRNA processing sites (*28*) and in the 5′-UTRs of mRNAs of genes related to cancer (*18*). In spite of the demonstrated role of the RNA G-quadruplexes, and the prevalence of sequences with the potential for forming G-quadruplexes, only a few such structures have been characterized. Given the widespread occurrence of the putative RNA G-quadruplex-forming sequences, it is not implausible to expect structural and functional diversity among them, especially if lessons are learned from the DNA G-quadruplex field. Thus, it is imperative that many such sequences need to be studied such that general principles on RNA G-quadruplex structure formation and their ability to control translation are adequately established.

Matrix metalloproteinases (MMPs) are zinc-dependent endopeptidases, which are capable of degrading extracellular matrix proteins (*29*, *30*). In particular, it has been shown that upregulation of MT3-MMP mRNA and the increase in the level of MMP protein expression are associated with the invasiveness of cancer cells (*31*), as in gastric cancer (*32*), prostate cancer (*33*, *34*), or

*To whom correspondence should be addressed. E-mail: sbasu@kent.edu. Telephone: (330) 672-3906. Fax: (330) 672-3816.

[1]Abbreviations: CD, circular dichroism; MMP, matrix metalloproteinase; mRNA, messenger ribonucleic acid; UTR, untranslated region.

Published on Web 04/28/2009

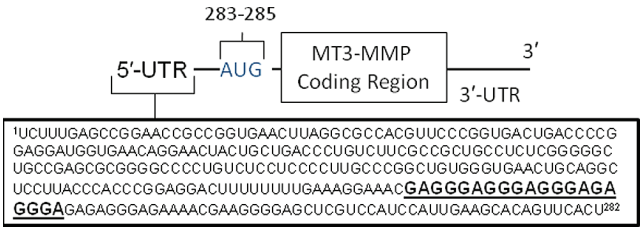

FIGURE 1: Schematic representation of MT3-MMP mRNA. The G-tracts of the G-quadruplex-forming sequence (M3Q) are shown in bold, and the translation start site is colored blue.

renal carcinoma (*35*), and with pathological processes such as angiogenesis in tumors (*36*, *37*). Despite the growing knowledge of the mechanism of MT3-MMP expression, its regulation at the translational level is not well delineated. The presence of a 20-nucleotide highly G-rich sequence (M3Q) comprised exclusively of purines and located upstream of the initiation codon (Figure 1) of MT3-MMP mRNA can be a potential regulator of its translation. Such G-rich sequences with multiple patches of contiguous guanosines are known to adopt three-dimensional folded forms (*18*, *23*, *26*). In this study, various biochemical and biophysical studies were performed to elucidate M3Q's ability to form a stable structure. Data obtained from CD spectroscopy, temperature-dependent melting, and enzymatic footprinting strongly suggest that this 20-nucleotide RNA sequence adopts a G-quadruplex structure with extremely high stability. A functional assay based upon measurement of dual luciferase activity performed in eukaryotic cells confirms the ability of the M3Q sequence in the context of the entire 282-nucleotide wild-type 5′-UTR of MT3-MMP to repress the expression of the reporter gene at the translational level.

MATERIALS AND METHODS

Preparation of Oligonucleotide Sequences. The RNA sequence 5′-rGAGGGAGGGAGGGAGAGGGA-3′ (M3Q) was purchased from Dharmacon, Inc. DNA templates used for in vitro transcription (*38*) of the RNA sequence 5′-rGAGAUAAGUGAGUGAGAGAGA-3′ (mut-M3Q) were purchased from Integrated DNA Technologies (IDT). RNA products were purified via denaturing 17% polyacrylamide gel electrophoresis (PAGE). Full-length products were visualized by UV shadowing and excised from the gel. The RNA was harvested via the crush and soak method by tumbling the gel slice overnight at 4 °C in a solution of 300 mM NaCl, 10 mM Tris-HCl, and 0.1 mM EDTA (pH 7.5). Salt was removed by ethanol precipitation of the RNA twice, with two 70% ethanol washes between each precipitation. The RNA pellet was dissolved in 10 mM Tris-HCl and 0.1 mM EDTA (pH 7.5). RNA concentrations were determined on the basis of their absorbance value at 260 nm and extinction coefficients calculated using nearest neighbor parameters (*39*).

5′-Labeling of RNA Oligonucleotides. The 5′-end phosphates of transcribed RNA were removed using calf intestinal alkaline phosphatase (New England Biolabs). CIP was removed by phenol extraction and subsequent ethanol precipitation using 20 μg of glycogen. The RNA was 5′-end-labeled by being treated with T4 polynucleotide kinase (Promega) and [γ-^{32}P]ATP (Perkin Elmer) and incubated for 45 min at 37 °C. The reaction was stopped by the addition of an equal volume of stop buffer [7 M urea, 10 mM Tris-HCl, and 0.1 mM EDTA (pH 7.4)]. The radiolabeled full-length RNA was isolated by 17% denaturing PAGE. The RNA was extracted from the gel via the crush and soak method as described above.

Circular Dichroism (CD) Studies. All measurements were recorded at room temperature. RNA was folded by heating the samples at various concentrations of KCl in 10 mM Tris-HCl and 0.1 mM EDTA (pH 7.5) at 97 °C for 5 min, followed by slow cooling to room temperature over a 90 min period. The circular dichroism (CD) spectra were recorded using a Jasco J-810 spectrophotometer with a 0.1 cm cell at a scan speed of 50 nm/min with a response time of 1 s. The spectra were averaged over five scans. For each sample, a buffer baseline was obtained in the same cuvette and subtracted from the average scan.

Melting Experiments. CD-melt spectra were recorded using a 0.1 cm path-length cell. Samples were prepared by heating oligonucleotides in 10 mM Tris-HCl and 0.1 mM EDTA (pH 7.5) in the presence of various salt and oligonucleotide concentrations at 97 °C for 5 min and then gradually cooled to room temperature at a gradient of 15 °C/h. Mineral oil was placed on top of the sample to prevent evaporation. The melting curves were obtained by monitoring a 263 nm CD peak. Thermodynamic parameters and T_m values were calculated using the van't Hoff method (*40*, *41*).

Footprinting by RNase T1. The 5′-end-labeled RNA was folded by heating the samples in the presence of various concentrations of KCl in 10 mM Tris-HCl and 0.1 mM EDTA (pH 7.5) at 97 °C for 5 min and then slowly cooled to room temperature. Once reaction mixtures reached room temperature, the RNA was digested with 0.5 units of RNase T1 (Ambion) for 5 min at room temperature. The reaction was terminated by using an equal volume of stop buffer as described previously.

Plasmid Construction. *(i) p-M3Q and p-G3A-M3Q*. p-M3Q and p-G3A-M3Q were inserted at the NheI site within the psiCHECK-2 vector (Promega) using the following oligonucleotides: M3Q-sense (5′-CTAGCGAGGGAGGGAGGGAGAGGGAA-3′), M3Q-antisense (5′-CTAGTTCCCTCTCCCTCCCTCCCTCG-3′), mut-M3Q-sense (5′-CTAGCGAAAAAGGGAGGGAGAGGGAA-3′), and mut-M3Q-antisense (5′-CTAGTTCCCTCTCCCTCCCTTTTTCG-3′). Ligated sequences were transformed into JM109 cells, and the plasmids were isolated. The insertion of the correct sequence was verified by sequencing performed at The Ohio State University's Plant-Microbe Genomics Facility.

(ii) wt-UTR and mut-UTR. The entire 282-nucleotide sequence of MT3-MMP (wt-UTR) was obtained from GenScript Corp., and the sequence was verified by the vendor. NheI sites were incorporated at the flanks of the segment for subsequent cutting and ligation into the psiCHECK-2 vector. A mutant (mut-UTR) was also purchased with the following base substitutions: G214A, G215U, G218U, G222U, and G228A. Ligated sequences were transformed, and the correctness of the sequence was verified as described above.

Cell Culture. HeLa cells were grown in 96-well plates in Dulbecco's modified Eagle's medium (DMEM) supplemented with 10% fetal bovine serum and the antibiotics streptomycin and penicillin at 37 °C in 5% CO_2 in a humidified incubator.

Dual Luciferase and Quantitative RT-PCR Assays. HeLa cells were transfected with plasmids described above using Lipofectamine 2000 (Invitrogen) according to the manufacturer's protocol. Twenty-four hours after transfection, Renilla (RL) and firefly (FL) luciferase activities were measured using a Dual-Glo Luciferase assay system (Promega) as per the manufacturer's supplied protocol on a Synergy 2 microplate reader (BioTek Instruments). Total RNA was extracted from transfected HeLa cells using a NucleoSpin RNA II kit (Clontech). Prior to reverse

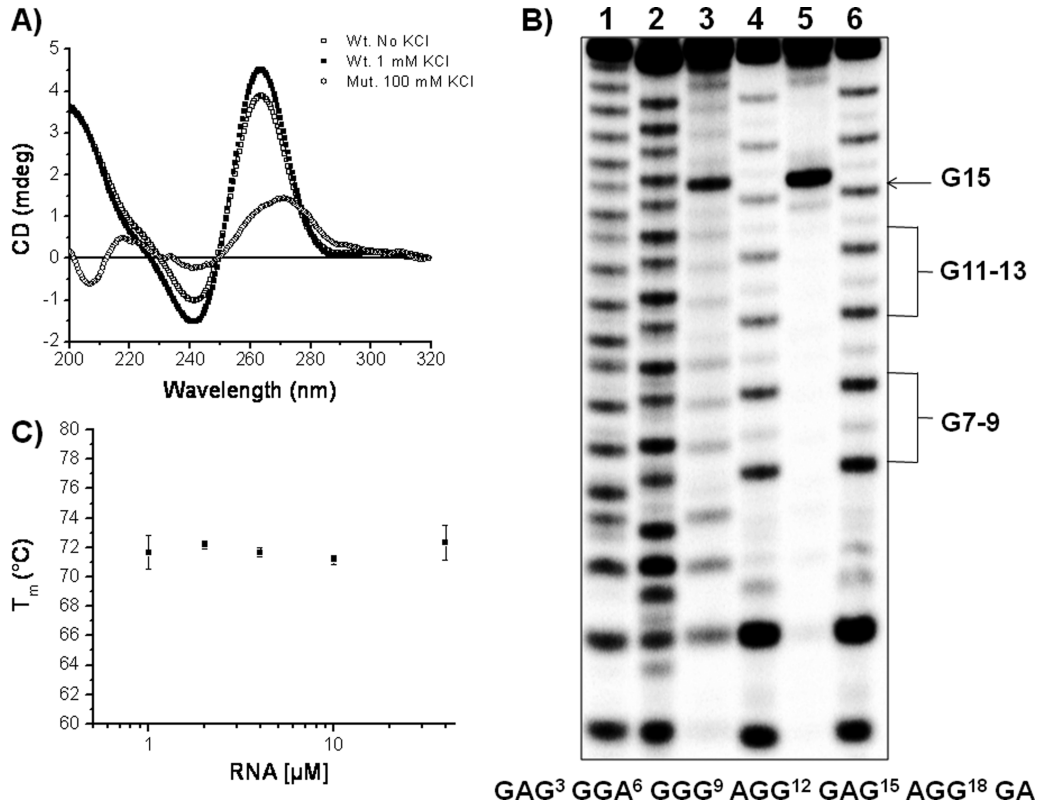

FIGURE 2: (A) Circular dichroism spectra of M3Q and mut-M3Q at a strand concentration of 5 μM in 0.1 mM EDTA and 10 mM Tris-HCl (pH 7.5) and in the presence of various concentrations of KCl. (B) RNase T1 footprinting of M3Q and mut-M3Q. Structures were preformed in 0 or 100 mM KCl and then incubated for 5 min at room temperature in the presence of 0.5 units of RNase T1. Lanes: base hydrolysis ladders for M3Q (lane 1) and mut-M3Q (lane 2), M3Q (lane 3) and mut-M3Q (lane 4) in the absence of KCl, and M3Q (lane 5) and mut-M3Q (lane 6) in the presence of 100 mM KCl. (C) Plot of T_m values for M3Q RNA at various strand concentrations. All experiments were conducted in 0.1 mM EDTA, 10 mM Tris-HCl (pH 7.5), and 1 mM KCl. (D) Proposed line drawing model for M3Q.

transcription, DNA was removed from each RNA sample upon treatment with RQ1 RNase-free DNase (Promega). Renilla and firefly mRNAs were reverse transcribed using AMV-RT (New England Biolabs), and cDNA was subjected to quantitative real-time PCR using a SYBR Green PCR Master Mix kit (Applied Biosystems) on an ABI PRISM 7000 Sequence Detection System in the presence of the appropriate set of primers: forward primers RL 5′-(GTAACGCTGCCTCCAGCTAC)-3′ and FL 5′-(TTCG CTAAGAGCACCCTGAT)-3′ and reverse primers RL 5′-(GTA GGCAGCGAACTCCTCAG)-3′ and FL 5′-(GCTGCAGCAG GATAGACTCC)-3′.

RESULTS

The M3Q Sequence Forms a Parallel G-Quadruplex Structure. To determine whether the G-rich M3Q RNA forms a structure, we used circular dichroism (CD) spectroscopy. A CD spectrum with a peak at 263 nm and a trough at 240 nm indicated that M3Q adopts a parallel G-quadruplex structure (*1*). Interestingly, M3Q generated a similar spectrum even in the absence of any added salt, suggesting an inherently strong propensity of the sequence to form a G-quadruplex, which has been previously reported (Figure 2A) (*18*). However, addition of 1 mM KCl increased the intensity of the CD spectrum at 263 nm, most likely due to enhanced G-quadruplex formation (*42*) and not because of any change in absorbance. It has been observed previously that the change in absorbance at 260 nm due to quadruplex formation is very small (~4%) (*43*, *44*), and thus, the change in the CD spectrum observed in Figure 2A can be ascribed to further stabilization of such structure and possibly more G-quadruplex formation.

It is well established that at least four consecutive G-rich stretches are required for formation of an intramolecular G-quadruplex (*1*). Changes to any of the G stretches should interfere with M3Q's ability to form an intramolecular G-quadruplex. A mutant sequence (mut-M3Q) in which base substitutions G214A, G215U, G218U, G222U, and G228A was designed with the expectation that such mutations would disrupt intramolecular G-quadruplex formation (*24*). Figure 2A shows the CD spectrum of mut-M3Q in the presence of physiologically relevant K^+ concentrations (100 mM KCl), and as expected, there were no noticeable features that can be attributed to G-quadruplex formation. Furthermore, the observed decrease in the intensity of the CD spectrum suggested a lack of helicity which suggests the presence of unstructured, single-stranded RNA (*45*).

A G-Quadruplex of Extreme Stability. To determine the stability of the structure formed by the M3Q RNA, CD melting experiments were performed by monitoring changes in CD intensity at 263 nm. Studies in the presence of 100 mM KCl showed no sign of melting of the structure even at temperatures above 95 °C, which forced us to measure the T_m values at lower K^+ concentrations. Figure 3 shows the CD melting curve of M3Q in the presence and absence of salt. In the absence of added salt, the structure begins to unfold just above the ambient temperature, resulting in a T_m of 38 ± 1 °C. However, addition of 1 mM KCl increased the T_m of the G-quadruplex by more than 30 °C (72 ± 1 °C). The T_m values determined by van't Hoff plots

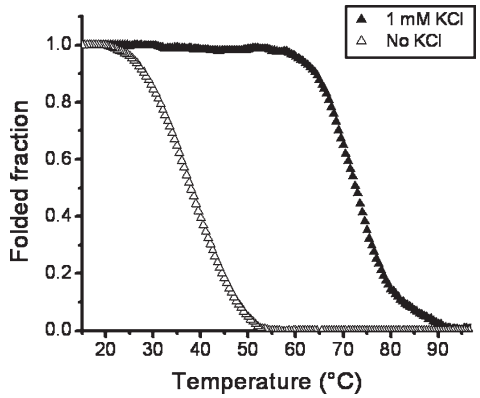

FIGURE 3: Circular dichroism melting curves of M3Q RNA at a strand concentration of 4 μM in 0.1 mM EDTA and 10 mM Tris-HCl (pH 7.5) in the presence of 0 and 1 mM KCl.

Table 1: T_m Values for M3Q RNA in the Presence of Various Cations

cation[a] (1 mM)	T_m (°C)
K^+	72
Na^+	45
Li^+	38

[a] For all experiments, the buffer consisted of 0.1 mM EDTA and 10 mM Tris-HCl (pH 7.5) in the presence of the indicated cation. T_m values are within ±1 °C.

Table 2: Thermodynamic Parameters for the Folding of M3Q

[KCl] (mM)	$\Delta H°$ (kJ/mol)	$\Delta S°$ (kJ mol^{-1} K^{-1})	$\Delta G°_{37°C}$ (kJ/mol)
0	−163 ± 7	−0.52 ± 0.03	−1.2 ± 0.6
1	−213 ± 20	−0.61 ± 0.07	−21.5 ± 2.7

and by first-derivative analyses agreed with each other quite well (data not shown). The annealing and melting curves showed reversible characteristics, which suggests that the molecules were at thermodynamic equilibrium (*41*). In the presence of various monovalent cations, M3Q showed the expected trend for G-quadruplex melting with T_m values in the following order: $K^+ > Na^+ > Li^+$ (Table 1) (*46*). The difference between Na^+ and K^+ is significant and most likely suggests a G-quadruplex structure.

Molecularity and Thermodynamic Properties of the G-Quadruplex. To determine the molecularity of the formed G-quadruplex, melting experiments were performed at various strand concentrations but under identical salt concentrations. The T_m remained unchanged as the M3Q concentration was varied from 1 to 40 μM (Figure 2C), which indicates intramolecular G-quadruplex formation (*18*, *44*, *47*). Thermodynamic parameters from the melting curves were calculated on the basis of a two-state model (folded → unfolded) (*40*, *41*). In the presence of 1 mM KCl, the Gibbs free energy ($\Delta G°$) at 37 °C increased 20-fold compared to the value in the absence of added salt (Table 2). The calculated $\Delta H°$ and $\Delta S°$ values (Table 2) compare well with previously reported values (*48*, *49*).

Footprinting on M3Q Shows Protection from RNase T1. To further probe the formation of G-quadruplex structure, footprinting experiments on M3Q and mut-M3Q were conducted with ribonuclease T1 (RNase T1). RNase T1 catalyzes cleavage at guanosines in single-stranded RNA, but not guanosines that

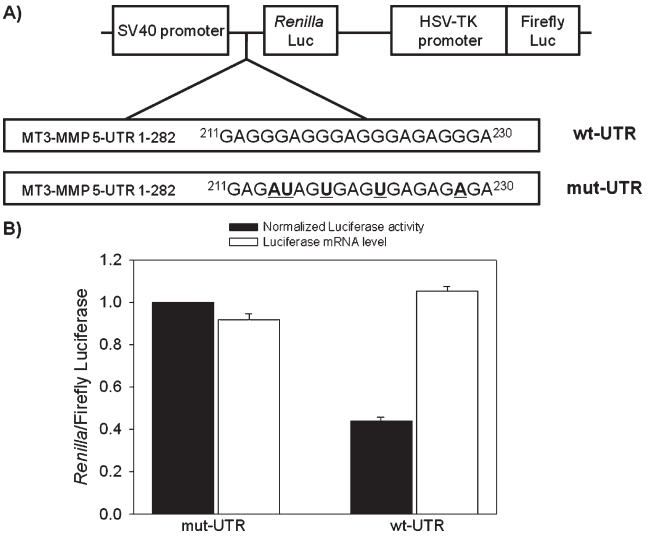

FIGURE 4: Dual luciferase reporter assay for demonstrating the role of the 5′-UTR of MT3-MMP on translation. (A) Schematic representation of the plasmids used to investigate the effect of the 5′-UTR of MT3-MMP on translation. (B) Histogram representing the ratio of Renilla to firefly luciferase activities in HeLa cells (black bars). The ratio of Renilla to firefly luciferase of the mut-UTR plasmid was set to one, and all other values were normalized accordingly. The ratio of CT values for Renilla to firefly determined by qRT-PCR (white bars). All experiments were conducted in triplicate at a minimum.

are present in the context of secondary or tertiary structures. Thus, guanosines that directly participate in quartet formation should be more protected from RNase T1-mediated cleavage compared to guanosines that are in the loop or the unstructured regions, and indeed, such patterns have been reported previously (*22*, *23*, *25*, *50*). Results from the footprinting experiment on M3Q showed that in the presence of 100 mM KCl, all guanosines except G1 (Figure 2B, not shown), a dangling end, and G15, which is apparently located within a single-stranded loop region, were protected (Figure 2B). In the absence of added salt, modifications were observed at all of the guanosines within the M3Q sequence at a slightly higher level compared to that observed in the presence of 100 mM KCl. This suggests that in the absence of added salt either a smaller fraction of M3Q was folded into a G-quadruplex structure or the overall population formed a less rigid structure. The observation is consistent with the CD spectrum in the absence of any added salt. However, RNase T1 footprinting on mut-M3Q in presence of 100 mM KCl resulted in no protection. All of the guanosine sites underwent cleavage under the experimental conditions, presumably due to the lack of structure formation. The data suggest that the M3Q RNA has a strong tendency to form an intramolecular G-quadruplex structure.

The M3Q Motif Inhibits Translation of a Reporter Gene in Eukaryotic Cells. To determine that the M3Q motif was responsible for translation inhibition in the context of the full-length wild-type 5′-untranslated region of MT3-MMP, the entire 282-nucleotide 5′-UTR or a mutated version (each G-run of M3Q strategically mutated; see Materials and Methods for details) was inserted upstream of the Renilla luciferase coding sequence in the psiCHECK-2 vector (wt-UTR and mut-UTR) and the resultant vectors were transfected into HeLa cells. When present in the context of the whole 5′-UTR, the M3Q sequence demonstrates inhibition of the reporter gene by 55% (Figure 4). However, the mutated version of the 5′-UTR (mut-UTR) did not affect translation at all. The mRNA levels of the reporter genes

remained unchanged as confirmed by qRT-PCR experiments. The results demonstrate that the M3Q G-quadruplex motif has the ability to inhibit gene expression by repressing translation of its mRNA.

To ensure that the G-quadruplex located in the 5′-UTR of MT3-MMP has an effect on translation, the M3Q or mutated M3Q sequence was also inserted upstream and in the proximity of the Renilla luciferase coding sequence in the psiCHECK-2 vector (p-M3Q) and transfected into HeLa cells (Figure S1 of the Supporting Information). Identical mutations in the G-quadruplex-forming motif in NRAS mRNA have been reported to disrupt G-quadruplex formation (*18*). Quantitation of the dual luciferase in HeLa cells showed inhibition of Renilla luciferase activity by 60%, while the mutated M3Q exhibited full activity (data not shown). To ensure the loss of activity is due to translation repression, we performed qRT-PCR experiments that showed no change in mRNA levels of either of the reporter genes. The ability of only the 20-nucleotide M3Q sequence and the M3Q sequence present in the context of the wild-type entire 5′-UTR to repress translation of a reporter gene by a similar amount suggests that this G-quadruplex motif is responsible for repression of translation.

DISCUSSION

Although many naturally occurring sequences have been predicted to form RNA G-quadruplexes (*18*, *28*), very few such structures and their functional relevance have actually been confirmed experimentally. Our data strongly suggest that a 20-nucleotide G-rich region in the 5′-UTR of MT3-MMP mRNA forms an extremely stable, intramolecular, parallel, G-quadruplex structure that can repress translation of a reporter mRNA. Formation of a parallel structure in an RNA G-quadruplex is expected, since an antiparallel CD spectrum would be unlikely due to the more favored C3′-endo conformation of the ribose ring (*51*), although a combination of C2′-endo and C3′-endo has also been observed (*52*). CD and enzymatic footprinting show that selected mutations (mut-M3Q) disrupt the formation of a G-quadruplex (Figure 2) (*24*). Such a disruption would be anticipated as it is well-known that the presence of four G-tracts in a single strand is an essential requirement for intramolecular G-quadruplex formation (*1*).

The M3Q sequence demonstrated remarkable stability and showed an increase in the T_m value of more than 30 °C upon the addition of 1 mM KCl, which is rather unexpected on the basis of the T_m values reported for biologically relevant RNA G-quadruplexes. In fact, at 5 mM KCl, the T_m increased by an additional ~10 °C (data not shown), suggesting that at the physiological K^+ concentration (~130 mM), unprecedented stability can be attributed to the M3Q RNA G-quadruplex structure. On the basis of the melting profile, thermodynamic parameters were calculated that provided an excellent basis for comparison of the stability of different structures. Reported values for biologically relevant RNA G-quadruplexes range from −39 to −50 kcal/mol, from −2.7 kcal/mol (at 37 °C) to −3.6 kcal/mol (at 25 °C), and from −100 to −130 cal/mol for $\Delta H°$, $\Delta G°$, and $\Delta S°$, respectively. These values calculated for M3Q in the presence of 1 mM KCl are in close agreement with those reported previously, but with a significant difference. The considerable difference that exists is between the conditions used to obtain the published values and conditions at which our experiments were performed, as our values were calculated from experiments performed at a ≥100-fold lower K^+ concentration (*53*−*55*). The ability of M3Q RNA to attain a thermodynamic stability on par with those of the reported RNA G-quadruplexes, despite being in a salt concentration 2 orders of magnitude lower, points toward its extreme stability. Such unusual stability can be rationalized due to some rather unique features present in the proposed G-quadruplex structure of M3Q RNA. To accommodate the single-nucleotide loops at positions 6 and 10, the putative folded structure must be compact and may also be thought to be not feasible due to strain in conformation. However, the presence of single-nucleotide loops in intramolecular G-quadruplexes has been observed in numerous previous studies (*18*, *26*, *48*, *49*, *56*, *57*). For example, in the C-MYC promoter DNA sequence, there is an inherent propensity for the selection of the G-tracts participating in the tetrad core to favor the formation of single-nucleotide loops, which suggested that such loops are the most stable "double-chain-reversal loops" that bridge three tetrads (*58*). G-Quadruplex stability is also linked to the actual number of short loops; it has been shown that increasing the number of such loops within a structure resulted in enhanced stability (*59*). The extreme stability of M3Q in comparison to other reported biologically relevant intramolecular RNA G-quadruplexes (*18*, *21*, *23*, *25*) may be the result of an additional single-nucleotide loop present in the M3Q structure as compared to other reported motifs. The adenine residues at positions 2 and 20 flanking the G-quadruplex core of M3Q may also contribute to its stability, as it has been found that dangling ends containing adenines stack particularly well to cap the G-quadruplex structures (*56*, *60*, *61*). For example, in a recent NMR study of the human telomere, it was found that adenine residues located in the loops and ends stacked and stabilized a G-quadruplex structure (*61*). Thus, the unique sequence of M3Q most likely contributes to its unprecedented stability.

Stable secondary RNA structures in the 5′-UTRs of mRNAs have been shown to regulate translation (*18*, *62*−*65*). In fact, RNA G-quadruplexes containing short or one-nucleotide loops have been found to be extremely stable and can inhibit translation (*18*, *26*, *47*). For example, an RNA G-quadruplex containing a $(G_3U)_n$ motif directly upstream of the Shine-Dalgarno sequence showed a very strong inhibition of translation of a reporter gene in bacteria (*26*). Furthermore, it has been shown in an in vitro assay that a G-quadruplex present in the human NRAS 5′-UTR, when inserted upstream of a reporter mRNA, reduced its translational efficiency (*18*). In eukaryotic cells, compelling evidence was found for the inhibitory role of a G-quadruplex-forming sequence present within the Zic-1 5′-UTR (*24*). In our study, the unusually stable G-quadruplex structure adopted by the M3Q sequence, present in the 5′-UTR of the MT3-MMP mRNA, showed a strong inhibitory role in translation, which is consistent with reports described above. However, most of the previous reports did not show the functional role of a G-quadruplex-forming sequence in the context of the native 5′-UTR in eukaryotic cells.

To investigate whether any secondary structure within the entire 5′-UTR can effectively compete with the formation of M3Q, we examined the sequence with QGRS Mapper (*28*) and mFOLD (*66*). QGRS Mapper revealed no putative G-quadruplex motifs within 100 nucleotides upstream of M3Q and two extremely weak ones beyond that point. Additionally, secondary structural analysis of the 40 flanking nucleotides on either side of M3Q using mFOLD resulted in a weak secondary structure with a predicted ΔG that is substantially higher than that calculated for M3Q folding (Table 2). From the investigation described

above, it seems highly unlikely that any G-quadruplex or other secondary structure could compete with M3Q G-quadruplex formation. Thus, the translational repression most likely can be attributed to the M3Q structure.

Since computational studies have predicted the presence of thousands of putative G-quadruplex-forming motifs in the 5′-UTR region of mRNAs (*18*), it is not far-fetched to expect structural and functional diversity in such motifs. To improve our understanding of the significance of these studies, it is imperative that such motifs be investigated to define their role in the regulation of translation. This work adds to our nascent knowledge of the role of G-quadruplex-forming RNA motifs in translation control. In light of these findings, particularly the demonstrated inhibitory role of the M3Q G-quadruplex, it may be postulated that yet to be identified cellular factors would have to unwind this very stable structure, thus facilitating translation of mRNAs with G-quadruplex motifs located in their 5′-UTR. Such a proposition may be more significant in case of certain types of cancers in which MT3-MMP expression is upregulated.

CONCLUSION

Herein, we have shown that M3Q forms an unusually stable intramolecular G-quadruplex that inhibits translation in eukaryotic cells. To the best of our knowledge, no intramolecular RNA G-quadruplex structure has been shown to be as stable as the M3Q structure at such low salt concentrations. The unique purine-only sequence of M3Q is likely stabilized via short nucleotide loops, the potential stacking of the flanking adenines, and the lack of competing intramolecular Watson−Crick base pairing. In general, this study supports the notion that RNA G-quadruplex motifs in the 5′-UTR can control translation and in particular begins to provide a molecular basis for translational regulation of MT3-MMP.

ACKNOWLEDGMENT

We thank Dr. Eric Wickstrom and J. D. Schonhoft for the critical reading and their comments on the manuscript.

SUPPORTING INFORMATION AVAILABLE

One figure showing a dual luciferase reporter assay to demonstrate the role of the M3Q sequence in translational control. This material is available free of charge via the Internet at http://pubs.acs.org.

REFERENCES

1. Neidle, S., and Balasubramanian, S. (2006) *Quadruplex Nucleic Acids*, RSC Biomolecular Sciences.
2. Gellert, M., Lipsett, M. N., and Davies, D. R. (1962) Helix formation by guanylic acid. *Proc. Natl. Acad. Sci. U.S.A. 48*, 2013–2018.
3. Sen, D., and Gilbert, W. (1988) Formation of parallel four-stranded complexes by guanine-rich motifs in DNA and its implications for meiosis. *Nature 334*, 364–366.
4. Williamson, J. R. (1994) G-Quartet structures in telomeric DNA. *Annu. Rev. Biophys. Biomol. Struct. 23*, 703–730.
5. Neidle, S., and Parkinson, G. N. (2003) The structure of telomeric DNA. *Curr. Opin. Struct. Biol. 13*, 275–283.
6. Gilbert, D. E., and Feigon, J. (1999) Multistranded DNA structures. *Curr. Opin. Struct. Biol. 9*, 305–314.
7. Huppert, J. L., and Balasubramanian, S. (2005) Prevalence of quadruplexes in the human genome. *Nucleic Acids Res. 33*, 2908–2916.
8. Eddy, J., and Maizels, N. (2008) Conserved elements with potential to form polymorphic G-quadruplex structures in the first intron of human genes. *Nucleic Acids Res. 36*, 1321–1333.
9. Huppert, J. L., and Balasubramanian, S. (2007) G-Quadruplexes in promoters throughout the human genome. *Nucleic Acids Res. 35*, 406–413.
10. Siddiqui-Jain, A., Grand, C. L., Bearss, D. J., and Hurley, L. H. (2002) Direct evidence for a G-quadruplex in a promoter region and its targeting with a small molecule to repress c-*MYC* transcription. *Proc. Natl. Acad. Sci. U.S.A. 99*, 11593–11598.
11. Simonsson, T., Pecinka, P., and Kubista, M. (1998) DNA tetraplex formation in the control region of c-myc. *Nucleic Acids Res. 26*, 1167–1172.
12. Dexheimer, T. S., Sun, D., and Hurley, L. H. (2006) Deconvoluting the structural and drug-recognition complexity of the G-quadruplex-forming region upstream of the bcl-2 P1 promoter. *J. Am. Chem. Soc. 128*, 5404–5415.
13. Cogoi, S., and Xodo, L. E. (2006) G-Quadruplex formation within the promoter of the KRAS proto-oncogene and its effect on transcription. *Nucleic Acids Res. 34*, 2536–2549.
14. Sun, D., Guo, K., Rusche, J. J., and Hurley, L. H. (2005) Facilitation of a structural transition in the polypurine/polypyrimidine tract within the proximal promoter region of the human VEGF gene by the presence of potassium and G-quadruplex-interactive agents. *Nucleic Acids Res. 33*, 6070–6080.
15. Cheong, C., and Moore, P. B. (1992) Solution structure of an unusually stable RNA tetraplex containing G- and U-quartet structures. *Biochemistry 31*, 8406–8414.
16. Kim, J., Cheong, C., and Moore, P. B. (1991) Tetramerization of an RNA oligonucleotide containing a GGGG sequence. *Nature 351*, 331–332.
17. Sacca, B., Lacroix, L., and Mergney, J.-L. (2005) The effect of chemical modifications on the thermal stability of different G quadruplex forming oligonucleotides. *Nucleic Acids Res. 33*, 1182–1192.
18. Kumari, S., Bugaut, A., Huppert, J. L., and Balasubramanian, S. (2007) An RNA G-quadruplex in the 5′-UTR of the NRAS proto-oncogene modulates translation. *Nat. Chem. Biol. 3*, 218–221.
19. Liu, H., Matsugami, A., Katahira, M., and Uesugi, S. (2002) A dimeric RNA quadruplex architecture comprised of two G:G(:A):G:G(:A) hexads, G:G:G:G tetrads and UUUU loops. *J. Mol. Biol. 322*, 955–970.
20. Sundquist, W. I., and Heaphy, S. (1993) Evidence for interstrand quadruplex formation in the dimerization of human immunodeficiency virus 1 genomic RNA. *Proc. Natl. Acad. Sci. U.S.A. 90*, 3393–3397.
21. Schaeffer, C., Bardoni, B., Mandel, J. L., Ehresmann, B., Ehresmann, C., and Moine, H. (2001) The fragile X mental retardation protein binds specifically to its mRNA via a purine quartet motif. *EMBO J. 20*, 4803–4813.
22. Darnell, J. C., Jensen, K. B., Jin, P., Brown, V., Warren, S. T., and Darnell, R. B. (2001) Fragile X mental retardation protein targets G quartet mRNAs important for neuronal function. *Cell 107*, 489–499.
23. Bonnal, S., Schaeffer, C., Creancier, L., Clamens, S., Moine, H., Prats, A.-C., and Vagner, S. (2003) A single internal ribosome entry site containing a G quartet RNA structure drives fibroblast growth factor 2 gene expression at four alternative translation initiation codons. *J. Biol. Chem. 278*, 39330–39336.
24. Arora, A., Dutkiewicz, M., Scaria, V., Hariharan, M., Maiti, S., and Kurreck, J. (2008) Inhibition of translation in living eukaryotic cells by an RNA G-quadruplex motif. *RNA 14*, 1290–1296.
25. Christiansen, J., Kofod, M., and Nielsen, F. C. (1994) A guanosine quadruplex and two stable hairpins flank a major cleavage site in insulin-like growth factor II mRNA. *Nucleic Acids Res. 22*, 5709–5716.
26. Wieland, M., and Hartig, J. S. (2007) RNA quadruplex-based modulation of gene expression. *Chem. Biol. 14*, 757–763.
27. Khateb, S., Weisman-Shomer, P., Hershco-Shani, I., Ludwig, A. L., and Fry, M. (2007) The tetraplex $(CGG)_n$ destabilizing proteins hnRNP A2 and CBF-A enhance the in vivo translation of fragile X premutation mRNA. *Nucleic Acids Res. 35*, 5775–5788.
28. Kostadinov, R., Malhotra, N., Viotti, M., Shine, R., D'Antonio, L., and Bagga, P. (2006) GRSDB: A database of quadruplex forming G-rich sequences in alternatively processed mammalian pre-mRNA sequences. *Nucleic Acids Res. 34*, D119–D124.
29. Egeblad, M., and Werb, Z. (2002) New functions for the matrix metalloproteinases in cancer progression. *Nat. Rev. Cancer 2*, 161–174.
30. McQuibban, G. A., Gong, J. H., Tam, E. M., McCulloch, C. A., Clark-Lewis, I., and Overall, C. M. (2000) Inflammation dampened by gelatinase A cleavage of monocyte chemoattractant protein-3. *Science 289*, 1202–1206.
31. Hotary, K., Li, X. Y., Allen, E., Stevens, S. L., and Weiss, S. J. (2006) A cancer cell metalloprotease triad regulates the basement membrane transmigration program. *Genes Dev. 20*, 2673–2686.

32. Lowy, A. M., Clements, W. M., Bishop, J., Kong, L., Bonney, T., Sisco, K., Aronow, B., Fenoglio-Preiser, C., and Groden, J. (2006) β-catenin/Wnt signaling regulates expression of the membrane type 3 matrix metalloproteinase in gastric cancer. *Cancer Res. 66*, 4734–4741.
33. Jung, M., Romer, A., Keyszer, G., Lein, M., Kristiansen, G., Schnorr, D., Loening, S. A., and Jung, K. (2003) mRNA expression of the five membrane-type matrix metalloproteinases MT1-MT5 in human prostatic cell lines and their down-regulation in human malignant prostatic tissue. *Prostate 55*, 89–98.
34. Daja, M. M., Niu, X., Zhao, Z., Brown, J. M., and Russell, P. J. (2003) Characterization of expression of matrix metalloproteinases and tissue inhibitors of metalloproteinases in prostate cancer cell lines. *Prostate Cancer Prostatic Dis. 6*, 15–26.
35. Kitagawa, Y. (1999) Expression of messenger RNAs for membrane-type 1, 2, and 3 matrix metalloproteinases in human renal cell carcinomas. *J. Urol. 162*, 905.
36. Stetler-Stevenson, W. G. (1999) Matrix metalloproteinases in angiogenesis: A moving target for therapeutic intervention. *J. Clin. Invest. 103*, 1237–1241.
37. Plaisier, M., Kapiteijn, K., Koolwijk, P., Fijten, C., Hanemaaijer, R., Grimbergen, J. M., Mulder-Stapel, A., Quax, P. H. A., Helmerhorst, F. M., and van Hinsbergh, V. W. M. (2004) Involvement of membrane-type matrix metalloproteinases (MT-MMPs) in capillary tube formation by human endometrial microvascular endothelial cells: Role of MT3-MMP. *J. Clin. Endocrinol. Metab. 89*, 5828–5836.
38. Milligan, J. F., Groebe, D. R., Witherell, G. W., and Uhlenbeck, O. C. (1987) Oligoribonucleotide synthesis using T7 RNA polymerase and synthetic DNA templates. *Nucleic Acids Res. 15*, 8783–8798.
39. Puglisi, J. D., Tinoco, I., James, E. D., and Abelson, J. N. (1989) Absorbance melting curves of RNA. *Methods in Enzymology*, pp 304−325, Academic Press, New York.
40. Marky, L. A., and Breslauer, K. J. (1987) Calculating thermodynamic data for transitions of any molecularity from equilibrium melting curves. *Biopolymers 26*, 1601.
41. Mergny, J.-L., and Lacroix, L. (2003) Analysis of thermal melting curves. *Oligonucleotides 13*, 515.
42. Nagatoishi, S., Tanaka, Y., and Tsumoto, K. (2007) Circular dichroism spectra demonstrate formation of the thrombin-binding DNA aptamer G-quadruplex under stabilizing-cation-deficient conditions. *Biochem. Biophys. Res. Commun. 352*, 812–817.
43. Mergny, J.-L., Phan, A.-T., and Lacroix, L. (1998) Following G-quartet formation by UV-spectroscopy. *FEBS Lett. 435*, 74–78.
44. Rachwal, P. A., and Fox, K. R. (2007) Quadruplex melting. *Methods 43*, 291.
45. Gray, D., Liu, J., Ratliff, R., and Allen, F. (1981) Sequence dependence of the circular dichroism of synthetic double-stranded RNAs. *Biopolymers 20*, 1337–1382.
46. Davis, J. T. (2004) G-Quartets 40 years later: From 5′-GMP to molecular biology and supramolecular chemistry. *Angew. Chem., Int. Ed. 43*, 668–698.
47. Risitano, A., and Fox, K. R. (2004) Influence of loop size on the stability of intramolecular DNA quadruplexes. *Nucleic Acids Res. 32*, 2598.
48. Rachwal, P. A., Brown, T., and Fox, K. R. (2007) Effect of G-tract length on the topology and stability of intramolecular DNA quadruplexes. *Biochemistry 46*, 3036–3044.
49. Rachwal, P. A., Brown, T., and Fox, K. R. (2007) Sequence effects of single base loops in intramolecular quadruplex DNA. *FEBS Lett. 581*, 1657–1660.
50. Xu, Y., Kaminaga, K., and Komiyama, M. (2008) G-Quadruplex formation by human telomeric repeats-containing RNA in Na^+ solution. *J. Am. Chem. Soc. 130*, 11179–11184.
51. Tang, C. F., and Shafer, R. H. (2006) Engineering the quadruplex fold: Nucleoside conformation determines both folding topology and molecularity in guanine quadruplexes. *J. Am. Chem. Soc. 128*, 5966–5973.
52. Deng, J., Xiong, Y., and Sundaralingam, M. (2001) X-ray analysis of an RNA tetraplex $(UGGGGU)_4$ with divalent Sr^{2+} ions at subatomic resolution (0.61 Å). *Proc. Natl. Acad. Sci. U.S.A. 98*, 13665–13670.
53. Menon, L., and Mihailescu, M.-R. (2007) Interactions of the G quartet forming semaphorin 3F RNA with the RGG box domain of the fragile X protein family. *Nucleic Acids Res. 35*, 5379–5392.
54. Marin, V. L., and Armitage, B. A. (2006) Hybridization of complementary and homologous peptide nucleic acid oligomers to a guanine quadruplex-forming RNA. *Biochemistry 45*, 1745–1754.
55. Zanotti, K. J., Lackey, P. E., Evans, G. L., and Mihailescu, M.-R. (2006) Thermodynamics of the fragile X mental retardation protein RGG box interactions with G quartet forming RNA. *Biochemistry 45*, 8319–8330.
56. Phan, A. T., Kuryavyi, V., Burge, S., Neidle, S., and Patel, D. J. (2007) Structure of an unprecedented G-quadruplex scaffold in the human c-kit promoter. *J. Am. Chem. Soc. 129*, 4386–4392.
57. Gao, N., Li, Y. H., Li, X., Yu, S., Fu, G. L., and Chen, B. (2007) Effect of α-synuclein on the promoter activity of tyrosine hydroxylase gene. *Neurosci. Bull. 23*, 53–57.
58. Phan, A. T., Modi, Y. S., and Patel, D. J. (2004) Propeller-type parallel-stranded G-quadruplexes in the human c-*myc* promoter. *J. Am. Chem. Soc. 126*, 8710–8716.
59. Rachwal, P. A., Findlow, I. S., Werner, J. M., Brown, T., and Fox, K. R. (2007) Intramolecular DNA quadruplexes with different arrangements of short and long loops. *Nucleic Acids Res. 35*, 4214–4222.
60. Matsugami, A., Okuizumi, T., Uesugi, S., and Katahira, M. (2003) Intramolecular higher order packing of parallel quadruplexes comprising a G:G:G:G tetrad and a G(:A):G(:A):G(:A):G heptad of GGA triplet repeat DNA. *J. Biol. Chem. 278*, 28147–28153.
61. Dai, J., Punchihewa, C., Ambrus, A., Chen, D., Jones, R. A., and Yang, D. (2007) Structure of the intramolecular human telomeric G-quadruplex in potassium solution: A novel adenine triple formation. *Nucleic Acids Res. 35*, 2440–2450.
62. Kozak, M. (1991) Structural features in eukaryotic mRNAs that modulate the initiation of translation. *J. Biol. Chem. 266*, 19867–19870.
63. Brenet, F., Dussault, N., Delfino, C., Boudouresque, F., Chinot, O., Martin, P. M., and Ouafik, L. H. (2006) Identification of secondary structure in the 5′-untranslated region of the human adrenomedullin mRNA with implications for the regulation of mRNA translation. *Oncogene 25*, 6510–6519.
64. Hess, M. A., and Duncan, R. F. (1996) Sequence and structure determinants of *Drosophila* Hsp70 mRNA translation: 5′-UTR secondary structure specifically inhibits heat shock protein mRNA translation. *Nucleic Acids Res. 24*, 2441–2449.
65. Manzella, J. M., and Blackshear, P. J. (1990) Regulation of rat ornithine decarboxylase mRNA translation by its 5′- untranslated region. *J. Biol. Chem. 265*, 11817–11822.
66. Zuker, M., Jaeger, J. A., and Turner, D. H. (1991) A comparison of optimal and suboptimal RNA secondary structures predicted by free energy minimization with structures determined by phylogenetic comparison. *Nucleic Acids Res. 19*, 2707–2714.